Chemical Engineering Science 285 (2024) 119591

Contents lists available at ScienceDirect

Chemical Engineering Science

journal homepage: www.elsevier.com/locate/ces

Design of sustainable reactor based on key performance indicators

Giuseppe Andriani [a], Benedetta A. De Liso [b], Gianmaria Pio [b], Ernesto Salzano [b,*]

[a] Università degli Studi di Padova, Dipartimento di Ingegneria Industriale, Via Marzolo 9, 35131 Padova, Italia
[b] Università di Bologna, Dipartimento di Ingegneria Civile, Chimica, Ambientale e dei Materiali, Via Terracini 28, 40131 Bologna, Italia

ARTICLE INFO

Keywords:
Reactor design
Key performance indicators
Scale-up
Sustainable processes
Runaway reactions

ABSTRACT

The design of chemical reactors has been largely considered primarily related to techno-economic evaluations. However, the recent need for sustainable solutions and processes has promoted the inclusion of environmental and safety parameters to identify the most suitable solution. In this sense, an innovative procedure has been developed in this work to identify and design a reactive section in chemical processes. To this aim, different key performance indicators have been defined and quantified for each domain considered within the analysis, namely technological, economic, environmental, and safety domains. In addition, the safety aspects have been quantified by integrating Semenov's theory and Varma, Morbidelli and Wu's theory. The validity and potentiality of the proposed procedure have been tested and shown by applying it to a case study representative for the scale-up of pharmaceutical processes: the industrial synthesis of a Vitamin A intermediate. A preliminary design has been performed for different configurations based on apparent kinetics determined from experimental data and ab initio coefficients available in the current literature. Among the analysed solutions, a single reactor with a volume of 15.90 m^3 has been indicated as the most suitable for the process requirements regarding overall sustainability. Hence, the developed procedure can be intended as a powerful tool for screening among available configurations, enabling a more informed decision by simplifying and optimising the scale-up and the detailed design.

1. Introduction

The accurate and robust design of reactors and the selection of optimised operative conditions represent a paramount step for developing sustainable chemical processes (Serna et al., 2016). This procedure requires the implementation of a multidisciplinary strategy to saturate the available degree of freedom and combine market requirements with physical–chemical constraints.

As an example, the geometrical configuration of a chemical reactor represents one of the most influential aspects to be identified at an early design phase (Froment et al., 2011). In addition, the number of units composing the reactive section in an industrial plant can be a matter of optimization. Typically, the design procedures available in the literature account mostly for technical requirements (Awad et al., 2022; Iezzi et al., 2022) or a combination of technical and economic aspects (Lagerman et al., 2022; Uddin et al., 2022). Conversely, the identification of the optimised operative conditions can result from an overall analysis of the industrial plant having as the main goal technical purposes (Chen et al., 2023; Ebadi et al., 2022) or techno-economic objectives (Torcida et al., 2022) or economic and safety points of view (Wu et al., 2023). In some cases, technical and safety aspects are strongly interconnected because the system's tendency to side (undesired) reactions is potentially detrimental to the selectivity toward the desired products or safety performances (e.g., runaway reactions).

An extensive set of alternative methodologies for selecting the best technical solution in the chemical industry is available in the current literature. More recently, particular effort has been devoted to individuating the most sustainable solution regarding economic, environmental and social aspects (Tugnoli et al., 2008). Despite all, practical applications to chemical process equipment are still rare. For example, quantitative multicriterial protocols have been involved in selecting separation technologies (Hutahaean et al., 2018), evaluating the best design of different equipment components and supply chains (Hodgett, 2016), or comparing various alternatives for energy production (Zanobetti et al., 2023). However, if considering reactor design, only a few examples of successfully implemented multicriteria approaches can be observed at the research stage, mostly related to selecting the optimal construction material for a particular reactor application (Martínez-Gómez & Narváez C, 2016).

* Corresponding author.
E-mail address: ernesto.salzano@unibo.it (E. Salzano).

https://doi.org/10.1016/j.ces.2023.119591
Received 19 September 2023; Received in revised form 2 November 2023; Accepted 30 November 2023
Available online 5 December 2023

Nomenclature

A	Heat transfer surface area
B	Dimensionless reaction enthalpy
C	Concentration in the overall liquid phase at the cooling temperature
$C_{A,in}$	Inlet concentration of the main reactant A
$C_{B,in}$	Inlet concentration of the main product B
$C_{B,out}$	Outlet concentration of the main product B
$\widehat{C}_p$	Heat capacity per unit mass
CAPEX	Capital expenditure
D	Impeller diameter
D_R	Reactor's diameter
Da	Damköhler number
DAB	1,4-diacetoxy-2-butene
E_a	Activation energy
$f(\chi)$	Mass action law
FAB	2-formyl-4-acetoxybutene
FOB	Free on board
H_R	Reactor's height
H_r	Ratio of the two reactions enthalpy
$\Delta\widetilde{H}_j$	Enthalpy of the j-th reactions per unit moles
k_k	Kinetic constant
$k_{k\infty}$	Arrhenius pre-exponential factor
N	Total number of CSTRs in series
n	Reaction order
$\dot{n}$	Molar flow rate
N_I	Impeller speed
N_{imp}	Numbers of impellers
$\dot{n}_B$	Productivity
$\dot{n}_{i,ex}$	Molar flow rate of the i-th compound exchanged between phases
$\dot{n}'''_{i,gen}$	Molar flow rate of the i-th compound generated per unit volume
N_{KPI}	Total number of categories considered for KPIs
$N_{\mathbb{P}}$	Power number
OPEX	Operational expenditure
P	Effective power consumption
P_{CO}	Partial pressure of CO
P_{H_2}	Partial pressure of H_2
$P_{ungassed}$	Power consumption of an ungassed system
$\dot{Q}$	Thermal power
$\widetilde{Q}_r$	Heat of reaction per unit moles
R	Dimensionless reaction rate
R_g	Universal gas constant
r	Total number of chemical reactions
$\mathscr{R}$	Dimensional reaction rate
R_r^{in}	Ratio of the two dimensionless reaction rates evaluated at the inlet condition
Re	Mixer's Reynolds number
RPD	Relative power demand
T	Reacting temperature
T_c	Critical temperature
T_{co}	Cooling temperature
T_{co}^{crit}	Critical value of the cooling temperature
T_s	Stable reaction temperature
U	Overall heat transfer coefficient
u	Dimensionless concentration
u_A	Dimensionless concentration of the main reactant A
u_{Ain}	Dimensionless inlet concentration of the main reactant A
u_B	Dimensionless concentration of the main product B
u_{Bin}	Dimensionless inlet concentration of the main product B
u_{Cin}	Dimensionless inlet concentration of the subproduct C
V	Reaction volume
$\dot{V}$	Volumetric flow rate
V_{aq}	Volume of the aqueous phase
V_{gas}	Volume of the gaseous phase
V_R	Reactor volume
$\dot{V}_{solvent}$	Volumetric flow rate of solvent
W	Impeller's width

Greek symbols

α_R	Aspect ratio
ε	Ratio of the gas phase volume respect to the reactor ones
ϵ	Aqueous phase hold-up
η	Yield
Θ	Dimensionless temperature of the reacting system
μ	Overall liquid phase viscosity
ν	Stoichiometric coefficient
ρ	Density
τ	Residence time
Y	Selectivity
χ	Conversion
ψ	Semenov's number
ω	Weighting factor

One of the critical aspects limiting the implementation of a multicriteria approach for reactor design, including safety and environmental factors, is represented by restrictions of the available models. Indeed, a standardised and robust procedure still needs to be made available for these two last-mentioned aspects. Regarding safety, conditions leading to a runaway reaction shall be considered when exothermic reactions are involved. Among the others, Semenov's theory of thermal explosion (ST) is worth mentioning. However, due to its assumptions, an approach based only on the ST has limited applicability to real cases. Indeed, ST can be mostly adopted to identify an inherently safe design of continuous stirred tank reactors (CSTR) (Babrauskas, 2014). Moreover, in its original derivation, ST can deal with only a single chemical reaction, which does not correspond to most real cases. The Varma Morbidelli and Wu theory of parametric sensitivity analysis (VMWT) can be considered as a possible alternative, although elevated computational requirements are typically associated with this approach (Varma et al., 1999). VMWT can be implemented for local or global sensitivity analyses based on the target's nature (Rabitz et al., 1983). Nevertheless, the application of VMWT is limited to simplified models, including a limited set of reactions and standardized mechanisms (e.g., reactions in series and/or in parallel) or an ideal chemical reactor.

Under these premises, the present work is devoted to the development and implementation of an innovative procedure for optimising the design of a chemical reactor that accounts for technical, economic, environmental, and safety requirements through a multicriteria selection procedure, which is based on the determination of internal normalised key performance indicators (KPIs) and an overall performance index. The single indicators are determined based on the numeric value of the characteristic variables for each single field of interest. These fundamental quantities are naturally obtained by applying the procedure elucidated subsequently.

A case study representative of a scale-up of vitamin A production is analysed to enlighten on the possible outcomes of the developed approach.

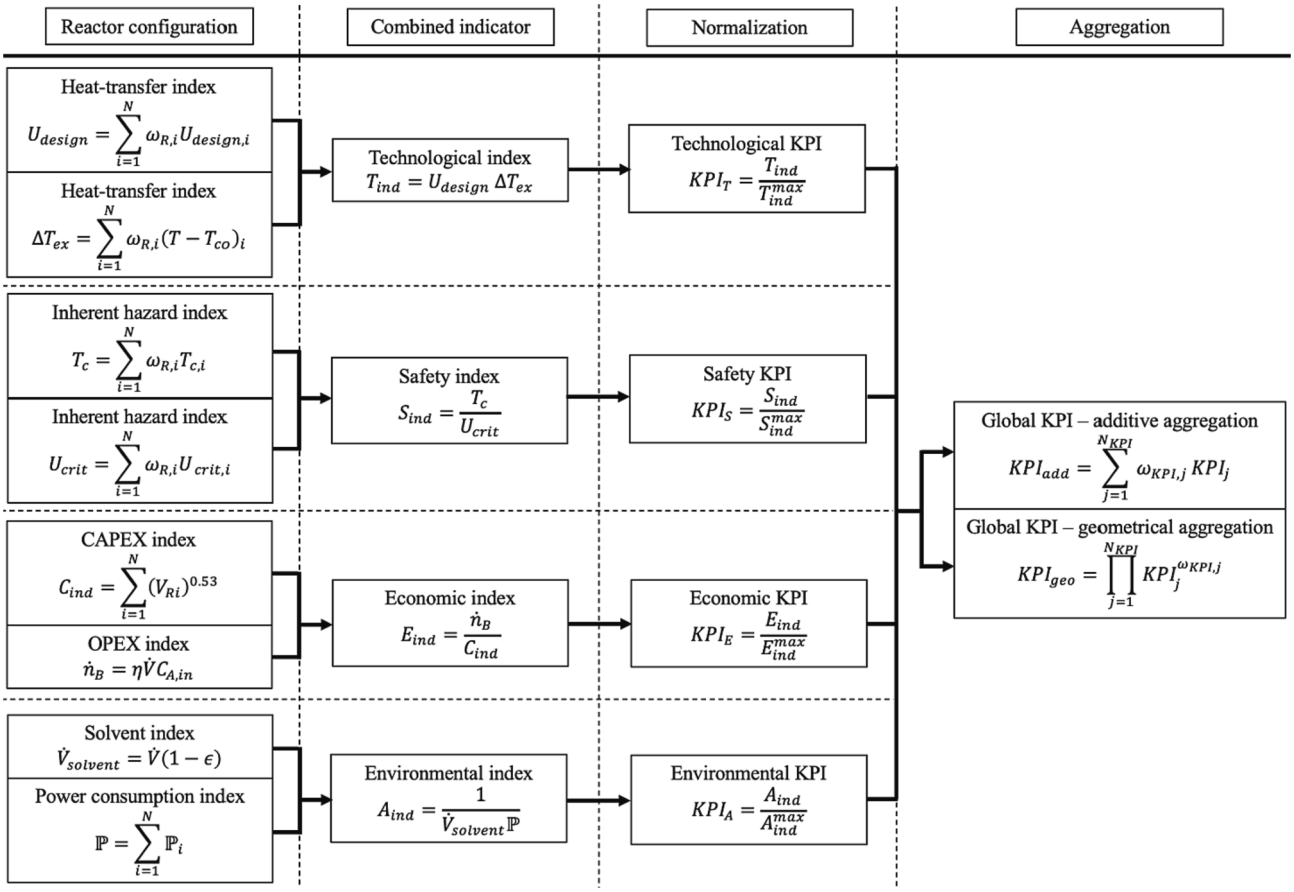

Fig. 1. Schematic representation of the considered key performance indicators.

2. Methodology

This work presents an innovative multicriteria procedure for the design of chemical reactors. Having different degrees of freedom, the design procedure can generate multiple alternatives. Hence, the best configuration among the others must be identified. To this aim, KPIs can simultaneously be adopted to evaluate different aspects (de Matos et al., 2023). KPIs can be intended as quantitative parameters describing the performances of a specific objective and domain, e.g., technological, safety, economic, and environmental. Hence, the calculation of overall KPIs can be used to rank the sustainability and convenience of possible alternative solutions. For clarity, a schematic representation of the implemented methodology is reported in Fig. 1. A brief highlight of the procedure is reported below, whereas a more detailed description is included in the following subsections.

The proposed method can be distinguished into four stages: determination of possible reactor configurations (Stage 1), recombination of indicators for specific domains (Stage 2), normalisation of KPIs to particular domains (Stage 3), and aggregation in an overall sustainability index (Stage 4). In Stage 1, the design of multiple possible reactor configurations is required. Although different levels of detail can be considered at this stage, the use of ideal reactor models is recommended to allow for the evaluation of a large set of alternative configurations. Assuming a continuous production process, plug flow reactors (PFR) and CSTR can be considered ideal configurations of chemical reactors. For simplicity, a general description of the characterisation of single CSTR and CSTRs in series is reported in detail. However, the design of a series of CSTRs can be considered an approach since PFR can be assumed to result from an infinite series of ideal CSTRs. The definition of boundary conditions and the resulting geometrical features of the reaction system determine the direct indicators (i.e., Stage 1 KPIs). A detailed description of this step and the adopted models is presented in Section 2.1. The obtained data are then recombined by domains, normalised, and aggregated in overall sustainability indexes to support the decision-making processes, following the procedure described in Sections 2.2, 2.3, and 2.4.

2.1. Determination of possible reactor configurations

A reference for ideal reactors must be selected to determine a preliminary configuration of the industrial process's chemical section. Considering the assumption of a continuous steady-state process, PFRs and CSTRs can be regarded as. In this sense, it is worth recalling that a PFR can also be intended as a series of infinite CSTRs. Under this consideration, the current methodology presents a detailed discussion on the optimisation of a series of CSTRs. For this purpose, a weighted average approach was implemented to obtain a single value by a series of N CSTRs, with a reactor weight coefficient $\omega_{R,i} = 1/N$. In the following part, the physical meaning and the derivation of the single variables will be elucidated. More specifically, the section named technological domain contains the procedure used to determine the overall heat transfer coefficient for the design U_{design} and the driving force for the heat exchange ΔT_{ex}. Whereas, the safety domain section includes the meaning and the procedure regarding the critical reaction temperature T_c and the critical value of the overall heat transfer coefficient U_{crit} together with the logical workflow used for the design based on the ST and VMWT. Then, in the economic domain section, a simplified methodology for determining CAPEX and OPEX will be described. Eventually, in the environmental domain section, the procedure for the assessment of the volumetric flow rate of the solvent $\dot{V}_{solvent}$ and the power consumption of the impeller motor $\mathbb{P}$ will be described.

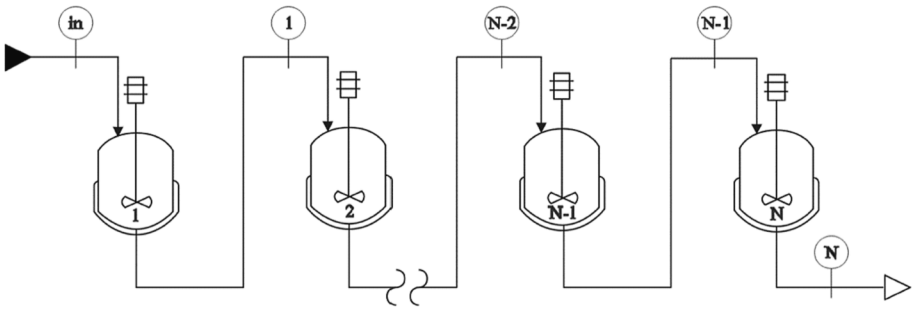

Fig. 2. Schematic representation of a series of CSTRs.

2.1.1. Technological domain

Starting with the design of a single CSTR, the ideal fluid dynamic model combined with the assumption of a constant density phase and steady-state operation leads to the dimensional mass and energy balance equations reported in Eqs. (1) and (2).

$$0 = \dot{V}\left(C_{i,in} - C_i\right) \pm \dot{n}_{i,ex} + \dot{n}''_{i,gen} V \tag{1}$$

$$0 = \rho \widehat{C}_p \dot{V}(T_{in} - T) - U_{design} A (T - T_{co}) + V \sum_{j=1}^{r} \left(- \Delta \widetilde{H}_j \right) \mathscr{R}_j \tag{2}$$

To this aim, the quantification of the surface area to be considered for heat exchange (A) is required. Based on the design stage, different approaches can be implemented for the estimation of this parameter. Assuming a possible lack of detailed information related to the application of this methodology in an early design stage, Eq. (3) can be considered for the estimation of A, under the hypothesis that heat transfer mostly occurs on the lateral surface wetted by the liquid. This approach requires the inclusion of a preliminary analysis of the reactor geometry (i.e., $\alpha_R = H_R/D_R, V_R = V_{liq} + V_{gas}$) and operative conditions (i.e., $\varepsilon = V_{gas}/V_R$ and $\epsilon = V_{aq}/V_{liq}$).

$$A = \frac{4^{2/3} \pi^{1/3} {\alpha_R}^{1/3} V_R^{2/3}}{1 + \varepsilon} \tag{3}$$

As for the overall heat transfer coefficient, since the specific geometry of the mixing and cooling systems is not known yet, the numerical value of this variable can't be determined based on fluid-dynamic features (Paul et al., 2004). Instead, it was considered a correlation based on the volume of the comprehensive liquid phase. Specifically, the empirical quadratic correlation reported in Eq. (4) is valid for steel reactors with a liquid volume phase between 2.5 and 25 m^3.

$$U_{calc} \left[W m^{-2} K^{-1} \right] = -0.9011 V_{liq}^2 - 7.363 V_{liq} + 1100.9 \tag{4}$$

Here, it is worth noting that Eq. (2) and the rest of the procedure do not consider U_{calc} but U_{design}. Indeed, even if both have the same physical meaning, their numerical values could be slightly different. The reason for this difference must be found in the ST, which states that a reactor operates safely if the curves of the heat removed and generated intersect each other for a reaction temperature equal to the one decided at the beginning of the procedure. Thus, the designer must verify this constraint after constructing Semenov's plot. If it is not confirmed, U_{calc} can't be increased but at least lowered till convergence is reached, obtaining U_{design}. In doing so, attention must be paid not to overcome the critical value defined in the following. This refinement can be considered legitimate since it can be obtained by acting, for example, on the impeller speed of the reactor.

Regarding the modelling strategy of a series of CSTRs, it is based on the minimisation of the total residence time $\tau_{tot} = V/\dot{V}$ needed to reach a desired conversion. For this reason, Eq. (5) can be considered an objective function to minimise by changing the intermediate conversion χ_m with $m = 1 \tilde{A} \cdot N - 1$. This last-mentioned equation is based on the mass balance of the main reactant A, considering the reference scheme reported in Fig. 2.

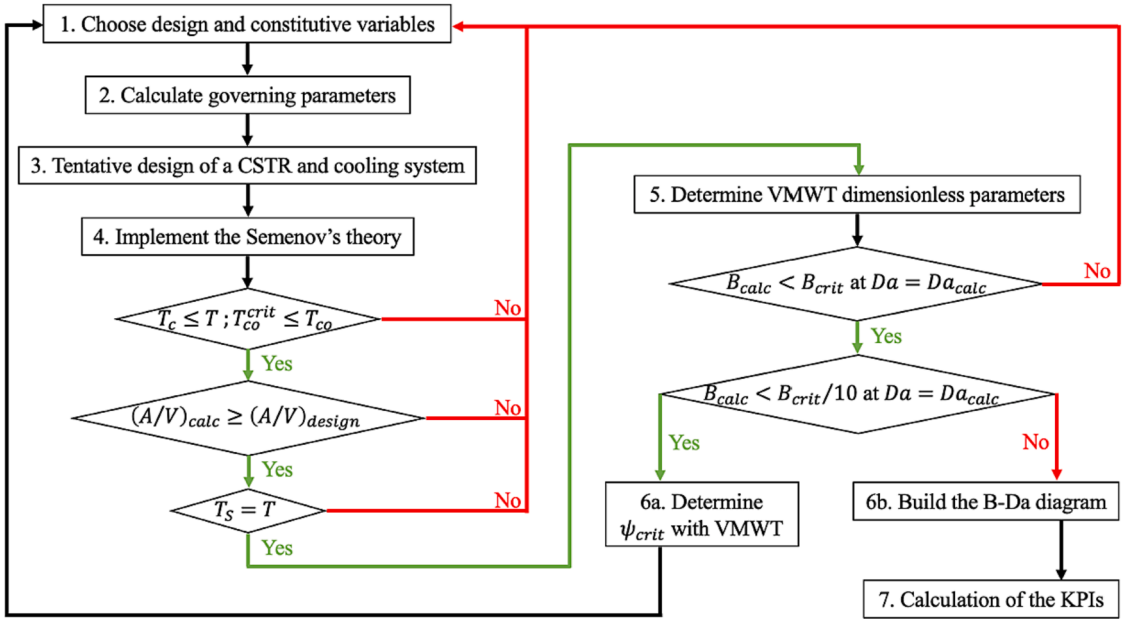

Fig. 3. Logical workflow for the design of a CSTR and cooling system using Semenov's theory and Varma, Morbidelli and Wu's theory.

$$\tau_{tot} = \sum_{k=1}^{N} \tau_k = \sum_{k=1}^{N} \frac{C_{A,in,k} - C_{A,k} \pm \frac{\dot{n}_{A,ex,k}}{\dot{V}}}{-\dot{n}''_{A,gen,k}} \tag{5}$$

2.1.2. Safety domain

At this stage, Semenov's theory and a modified parametric sensitivity were combined to identify the most critical parameters and KPIs, as schematised in Fig. 3.

Step 1 of the procedure implemented in this work aims to select the main input parameters. Among the others, the reaction temperature, the volumetric flow rate, and the initial concentrations can be considered governing parameters. Based on the assumed values, the main physicochemical parameters are calculated at the desired operating conditions (Step 2), and a tentative design configuration for reactor(s) and cooling system(s) is produced at this stage using Equations (1), 2 and 4 (Step 3). Once the preliminary phase is concluded, Semenov's theory is implemented (Step 4) by producing a Semenov plot at first. Then, the critical temperature (T_c, Eq. (6)), the critical value of the overall heat transfer coefficient (U_{crit}, Eq. (7)) and the critical temperature of the cooling medium (T_{co}^{crit}, Eq. (8)) are calculated. Starting from the classical ST, a kinetic rule suitable for the main nth-order exothermic reaction was introduced (Eq. (9)). Considering critical conditions and the classical value for the critical Semenov's number $\psi_{crit} = 1/e$, $(A/V)_{crit}$ was obtained, at first. From this critical ratio, a design value $(A/V)_{design}$ was obtained, considering a safety factor of 0.2. The safety factor was selected in agreement with the value commonly adopted for the design of pressurized vessels and auxiliary equipment items (Ennis, 2006).

$$\frac{R_g}{E_{a1}} T_c^2 - T_c + T_{co} = 0 \tag{6}$$

$$U_{crit} = \frac{\dot{Q}_{gen}\Big|_{\chi \to 0, T_c}}{(T_c - T_{co})A} \tag{7}$$

$$\dot{Q}_{ex}^{crit1} = U_{design} A \left(T_c^{'} - T_{co}^{crit}\right) \tag{8}$$

$$\psi = \frac{\widetilde{Q}_{r1} V C_{A,in}^{n_1} k_{k1\infty} \exp\left[-\frac{E_{a1}}{R_g T_{co}}\right]}{A U_{design}} \frac{E_{a1}}{R_g T_{co}^2} \tag{9}$$

Further refinements were considered by implementing the VMWT to the analysed reactive system (Step 5). In this work, the dimensionless reactor outlet temperature and the dimensionless heat of the reaction were considered as the measurable for the sensitivity analysis, as reported in Eq. (10). To this aim, the VMWT was modified to include multiple reactions and CSTRs within the numerical model adopted for the analysis required to determine B_{crit}. For brevity, the obtained equations are reported in the Supplementary materials for the case of two chemical reactions in series (i.e., $A \rightarrow B \rightarrow C$) together with the sensitivity equations.

$$S(\Theta; B) = \frac{B}{\Theta} s(\Theta; B) \tag{10}$$

A refined critical Semenov's number can also be calculated based on the obtained B_{crit} (Step 6a) using Eq. (11).

$$\psi_{crit} = \frac{Da\, B_{crit}}{St} \tag{11}$$

In this way, an optimised configuration can be obtained through an additional iteration of the method, assuming a more robust $(A/V)_{design}$. On the one hand, the optimised configuration can achieve higher performance making better use of the reaction volume. On the other hand, the B value shall be carefully evaluated to monitor the proximity to the critical one. Eventually, the performances of the resulting configurations can be quantified in terms of a reactor operation diagram (Step 6b). To build the reactor operation diagram, the critical values of B must be obtained as a function of the Da number. Additional information can be gathered if the corresponding values of yield and selectivity are assessed. The maximum yield and selectivity are determined for a B value equal to the one above which runaway occurs. Eventually, in Step 7 KPIs are determined following the procedure reported in Section 2.1.

2.1.3. Economic domain

The evaluation of the KPI related to the economic domain is based on the assessment of CAPEX and OPEX at an early design stage. Regarding the CAPEX estimation of the CSTRs, a simplified method based on the equipment characteristic size has been adopted. In particular, Eq. (12) was employed for a FOB cost estimation (Woods, 2007).

$$FOB = FOB_{reference} \left(\frac{V_R}{V_{R,reference}}\right)^{0.53} \tag{12}$$

On the other hand, the revenues and OPEX are typically associated with the production rate, feed or utility flow rates (Sinnott & Towler, 2020). The fluctuations in their costs can significantly affect the robustness of OPEX estimation. For these reasons, in the present work, a simplified analysis was performed considering only productivity, namely the main constituent of profitability. Strictly speaking, productivity is an economic index accounting for the positive feedback deriving from the productivity level, thus it is compared to the inverse of the indicator considered for the CAPEX. For the sake of clarity, the definition of productivity $\dot{n}_B$ is reported in Equation (13), considering η as the yield in the desired product.

$$\dot{n}_B = \eta \dot{V} C_{A,in} \tag{13}$$

2.1.4. Environmental domain

Since the separation sections are typically the most demanding in terms of energy and material in many manufacturing processes (Anastas & Zimmerman, 2003), outlet purity was regarded as a possible indicator of the environmental impact. More specifically, the higher will be the stream flow rate to purify, and the higher will be the effect of the operation on the environment. In chemical processes, the reactions are often performed in undesirable solvents, typically chlorinated or aromatic hydrocarbons (Sheldon et al., 2002). The green technology facilitates the minimum use of non-hazardous media (Dai et al., 2013), hence solutions that minimize the use of such liquids are preferred. To this aim, the volumetric flow rate of organic solvent was also considered.

The other constituent of the environmental domain is related to the power consumption of the reactor's impeller motor. Indeed, in CSTRs this term is one of the primary energy requirements and must be considered. To perform this estimate, the ratio between the impeller and reactor diameter must be chosen together with the impeller type and the Reynolds number (Luong & Volesky, 1979). After that, the impeller speed can be determined using Eq. (14), which is based on the definition of the Reynolds number of mixers.

$$N_I = \frac{Re\, \mu_{liq}}{\rho_{liq} D^2} \tag{14}$$

Using a classical flow map that relates the power number as a function of the Reynolds number for different types of turbines, it is possible to obtain the power number $N_{\mathbb{P}}$. Now the power consumption can be determined considering that, for sufficiently spaced turbines, Eq. (15) can be used (Furukawa et al., 2019).

$$\mathbb{P}_{ungassed} = N_{imp} N_{\mathbb{P}} \rho_{liq} N_I^3 D^5 \tag{15}$$

The above-reported relationship is valid for mixers that handle only liquid phases. To determine the power consumption for a gas/liquid system, an RPD value must be used. This variable relates the power absorbed by the impeller in the presence of the gaseous phase to the ungassed system. Eq. (16) reports the expression for the final determination of the effective power consumption in the case of a multiphase

gas/liquid system.

$$\mathbb{P} = RPD\,\mathbb{P}_{ungassed} \tag{16}$$

2.2. Assessment of combined indicators

The recombination of indexes accounting for the same domain is performed at this stage. The adopted equations were determined following a physical meaning, if possible, as well as to guarantee that the larger the value, the better the performance. To be more specific, the technological indicator is directly proportional to both the overall heat transfer coefficient and the heat transport driving force. Indeed, the higher the numerical value of the two last-mentioned variables, the higher the suitability of the temperature management system. Therefore, the provided definition of the technological indicator is intended as a combination of elements accounting for the quality of design. Regarding safety, the indicator is directly proportional to the critical reaction temperature and inversely proportional to the critical value of the heat transfer coefficient because higher T_c and lower U_c values mean minor thermal hazards. In the economic indicator, the factor accounting for the production level is divided by the CAPEX index, representing positive and negative impacts on the economic aspects, respectively. Eventually, from the environmental perspective, either the flow rate of solvent or the energy consumption inversely contributes to the index since in both cases large values imply lower compatibility of the proposed process.

2.3. Normalization of KPIs

An internal normalization step is performed at this stage for the sake of comparisons between different domains. Following the approach discussed in the previous subsection, the higher the numerical value of each normalized index, the higher the associated performance of the current solution in the related domain.

2.4. Evaluation of overall sustainability indexes

For the evaluation of the overall sustainability index, two aggregation approaches were implemented to test the robustness of the selected solution. More specifically, the sustainability indicators from the proposed analysis were obtained using additive and geometrical aggregation methods with equal weighting factors for KPIs deriving from different domains ($\omega_{KPI,j} = 1/N_{KPI}$) (Gan et al., 2017). Indeed, equal weighting is recommended when all the indicators are considered equally important or when no statistical or empirical evidence supports a different scheme (Nardo et al., 2005).

3. Case study

The proposed methodology was tested for the case of the industrial synthesis of a vitamin A intermediate, i.e., retinyl acetate. Currently, the most convenient route for its production is based on the BASF and Hoffman-La Roche process via two different reaction pathways (Parker et al., 2016). A new synthesis route, involving a water-soluble Rh complex catalyst, has been proposed and experimentally tested on a bench scale by Chansarkar et al. (Chansarkar et al., 2003). Data collected by Chansarkar et al. (2003) were adopted to quantify the kinetic parameters reported in Eq. (16). The resulting kinetic parameters were considered to design continuous equipment for the hydroformylation of 1,4-diacetoxy-2-butene (DAB) to 2-formyl-4-acetoxybutene (FAB). For the sake of conciseness, a detailed description of the additional assumptions posed and constituent parameters involved for the hydroformylation is reported in the Supplementary materials.

Considering the operative conditions examined during the cited experimental campaign (i.e., 338 K–358 K), the following analysis was performed within the same interval to avoid extrapolations. Based on

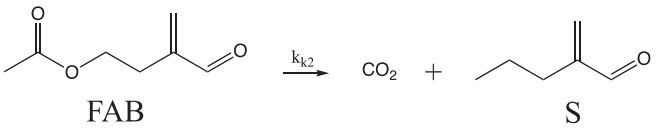

Fig. 4. Schematic representation of the liming reaction of the decomposition mechanism.

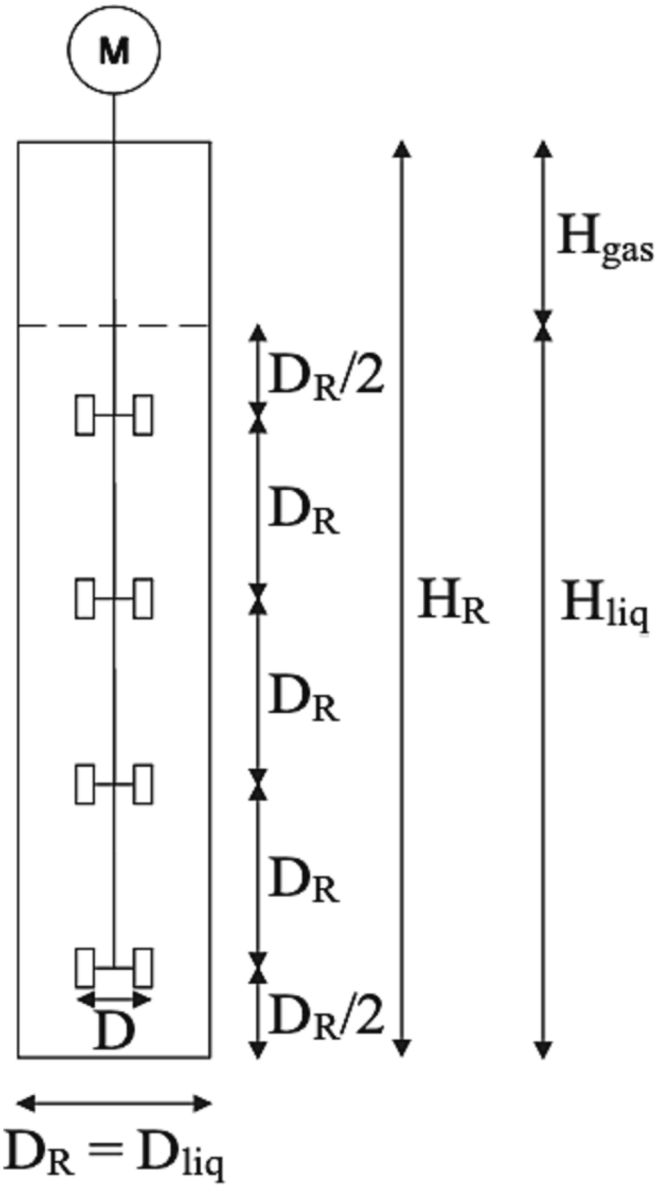

Fig. 5. Sketch of the proposed reactor geometry.

the operative conditions of interest, a decomposition mechanism was produced and included in the analysis. To this aim, the key elementary chemical reaction steps connecting the raw materials with possible products were identified by employing the Reaction Mechanism Generator suite (Gao et al., 2016). This database can be intended as a possible route for the collection of required input data in the case of missing or lacking kinetic parameters as well as for the generation of theoretical-based, robust, and detailed kinetic mechanisms (Pio et al., 2022). The potential use of kinetic mechanisms for the evaluation of real-case industrial processes has been already demonstrated in the current literature (Pio & Salzano, 2020) (De Liso et al., 2023). Based on

Table 1
Main characteristics of the obtained reactor configurations.

#Solution	N	T_{co}	T_c	U_{design}	U_{crit}	χ	$\dot{V}$	V_R	D_R	$C_{A,in}$
	–	K	K	$\frac{W}{m^2K}$	$\frac{W}{m^2K}$	–	$\frac{m^3}{s}$	m^3	m	$\frac{kmol}{m^3}$
1	1	348	371	678	495	0.685	$5\,10^{-3}$	21.10	1.75	0.275
	2	348	371	350	251	0.928	$5\,10^{-3}$	15.60	1.58	0.086
	3	348	371	150	106	0.990	$5\,10^{-3}$	10.70	1.40	0.025
2	1	345	368	665	577	0.685	$4\,10^{-3}$	21.95	1.90	0.465
	2	345	368	335	293	0.928	$4\,10^{-3}$	16.22	1.72	0.146
	3	345	368	140	123	0.990	$4\,10^{-3}$	11.14	1.52	0.033
3	1	348	371	901	658	0.685	$2\,10^{-3}$	13.24	1.50	0.677
	2	348	371	457	334	0.928	$2\,10^{-3}$	9.78	1.36	0.213
	3	348	371	141	141	0.990	$2\,10^{-3}$	6.72	1.20	0.049
4	1	348	371	925	676	0.851	$1\,10^{-3}$	12.41	1.47	0.730
	2	348	371	306	224	0.990	$1\,10^{-3}$	7.81	1.26	0.109
5	1	348	371	1013	741	0.851	$5\,10^{-4}$	7.90	1.26	1.185
	2	348	371	336	245	0.990	$5\,10^{-4}$	4.98	1.08	0.176
6	1	347	370	635	469	0.990	$7\,10^{-4}$	23.48	1.82	0.265
7	1	345	368	846	740	0.990	$2.5\,10^{-4}$	15.90	1.59	0.950
8	1	347	370	520	390	0.990	$1\,10^{-3}$	25.32	1.86	0.151

the corresponding kinetic coefficients, the rate-determining steps were selected following the procedure described in the literature (Pio et al., 2019). The rate-determining step of the decomposition mechanism is reported in Fig. 4, whereas the kinetic coefficients deriving from the rate-rule method, as included within the RMG database (Gao et al., 2016), are reported in Eq. (17).

$$\mathscr{R}_2\left[kmol\,m^{-3}s^{-1}\right] = 1.76\,10^8\,T^{1.63}\exp\left[-\frac{4.21\,10^4}{T[K]}\right]C_{FAB} \tag{17}$$

Considering a steady-state operation, the reactive volume can be assumed equal to the organic liquid phase. Then, the overall liquid volume can be calculated using the aqueous phase hold-up and the global reactor volume can be determined considering the gaseous hold-up (Jagani et al., 2010). This study assessed an aspect ratio of 5, a gaseous hold-up of 0.2, and an impeller with a diameter equal to 1/3 of the reactor diameter (Bao et al., 2015). Moreover, a pitched blade impeller type with six blades and $D/W = 8$ has been selected together with a Reynolds number equal to 200 000 (Paul et al., 2004) to ensure a turbulent flow and an $N_{\mathbb{P}} = 1.5$. Finally, an $RPD = 0.9$ has been assumed, considering a low gas flow dimensionless number, or rather a low gas flow rate fed to the system. For the sake of clarity, Fig. 5 reports a generic sketch of the proposed reactor geometry, which represents the configurations obtained in this work.

3.1. Application of the methodology

For the sake of clarity, the kinetic parameters for the hydroformylation reaction of DAB derived from the experimental data and assumptions described in the current literature (Chansarkar et al., 2003) are reported in Eq. (18).

$$\mathscr{R}_1\left[kmol\,m^{-3}s^{-1}\right] = 8.71\,10^6 \bullet \exp\left[-\frac{5.92\,10^3}{T[K]}\right]C_{cat}\frac{C_{H_2(T)}}{C_{CO(T)}}C_{DAB}^{0.5} \tag{18}$$

It is worth mentioning that the reaction rate of hydroformylation reported in Eq. (16) can be directly or inversely proportional to the concentration of carbon monoxide depending on its partial pressure, as reported by Chansarkar et al. (2007). Assuming the partial pressure of carbon monoxide used to maximise the reaction rate (i.e., equal to 3.40 MPa), an inversely proportional relationship has been selected. It should be noted that the Damköhler number and the outcomes of the design procedure are independent of the choice of the reaction rate expression since the overall reaction rate is considered.

Based on the conditions of interest for the analysed process, calculated and literature data, eight configurations were designed, and their outcomes are reported in Table 1. The reaction temperature was considered a common basis, with the overall conversion value equal to 358 K and 0.990, respectively. During the design procedure, the minimum acceptable difference between the cooling and reaction temperatures was 10 K. The defined KPIs were calculated from the obtained data (Fig. 6), following the described methodology. For conciseness, the detailed calculation procedure implemented to obtain the values reported in Table 1 is reported in Supplementary Materials.

The technological and the safety domains are mainly dependent on the thermal features of the systems, whereas the economic and the environmental ones depend on the liquid volumetric flow rate and the use or not of a series of CSTRs. Starting from the technological point of view, Solution 7 shows the highest value of KPI_T since it can most efficiently dispose of the thermal energy generated by the exothermic reactions. On the other hand, from the safety perspective, Solution 1 reduces the thermal hazards linked to the operation regarding the critical values of reaction temperature and overall heat transfer coefficient. Regarding the economic domain, instead, Solutions 5 and 3 have practically the same performances, even if the 5th alternative allows us to reach a better compromise between CAPEX and productivity. Due to the explicit dependence on reactor volume, CAPEX is strongly affected by the total residence time, which in turn depends on the volumetric flow rate and reactor type. In fact, because of the intrinsic nature of the hydroformylation and decomposition reactions, a PFR would have been the ideal choice but is not suitable for a liquid/liquid/gas application. Using a single CSTR, instead of only using a low volumetric flow rate, is possible to have restrained reactor volumes. While, with a series of CSTRs, the influence of the residence time on each reaction volume is reduced, and it is possible to increase the liquid stream flux. In this way, higher productivity and higher economic indexes are also reached. Conversely, a higher volumetric flow rate also means more elevated amounts of the organic phase, hence higher environmental impacts. In addition, in a series of CSTRs, higher power demand is also needed for the mixing operation. Thus, the lowest KPI_A is associated with these solutions. Finally, although different values can be observed based on the analysed aggregation method, the additive or geometrical aggregation methods indicate Solution 7 as the best configuration. Hence, Semenov's plot (Fig. 7) and the stability diagram (Fig. 8) are reported only for this configuration.

Semenov's plot demonstrates the stability operations of the analysed solution, being the thermal power generated and thermal power exchanged equally at the reaction temperature. Moreover, it can also be observed that the U_{design} and T_{co} values are respectively larger and lower than the critical ones, avoiding a metastable operation represented by

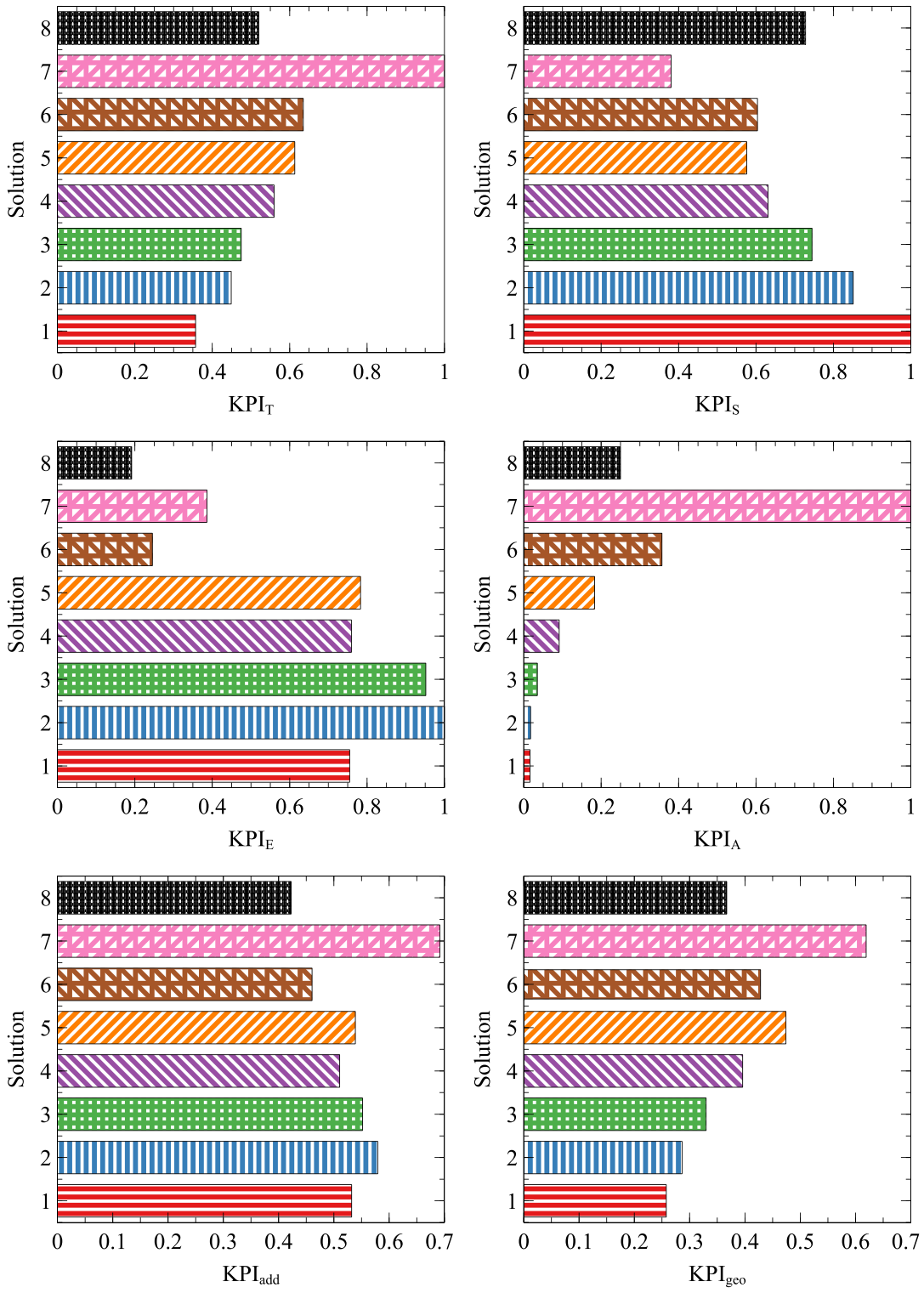

Fig. 6. Key Performance Indicators obtained for the configurations analysed in this work.

the two mentioned tangency conditions. On the other hand, as it can be noticed from the reactor operation diagram, the maximum achievable selectivity tends to be 1 since the second reaction occurs in series and has a slower rate at the investigated conditions than the main reaction. Moreover, the CSTR cannot undergo runaway reactions as long as the design specifications are satisfied since *Da* and *B* values for each reactor are under the safe-runaway transition limit. Being the *Da* and *B* values lower than the critical values, the yield calculated employing the VMWT is lower than the reported value in the safe-runaway transition curve. This is a consequence of the fact that the reactor is operating safely. Indeed, since the *B* value is below the critical one, the reaction temperature is under the value at which a runaway occurs. Consequently, the reaction rates are affected, limiting conversion and yield for a fixed *Da* value. Remarkably, a significant variation in the yield trend at the safe-runaway transition curve can be observed. This variation can be attributed to the proximity of Damköhler number to 0.1, corresponding

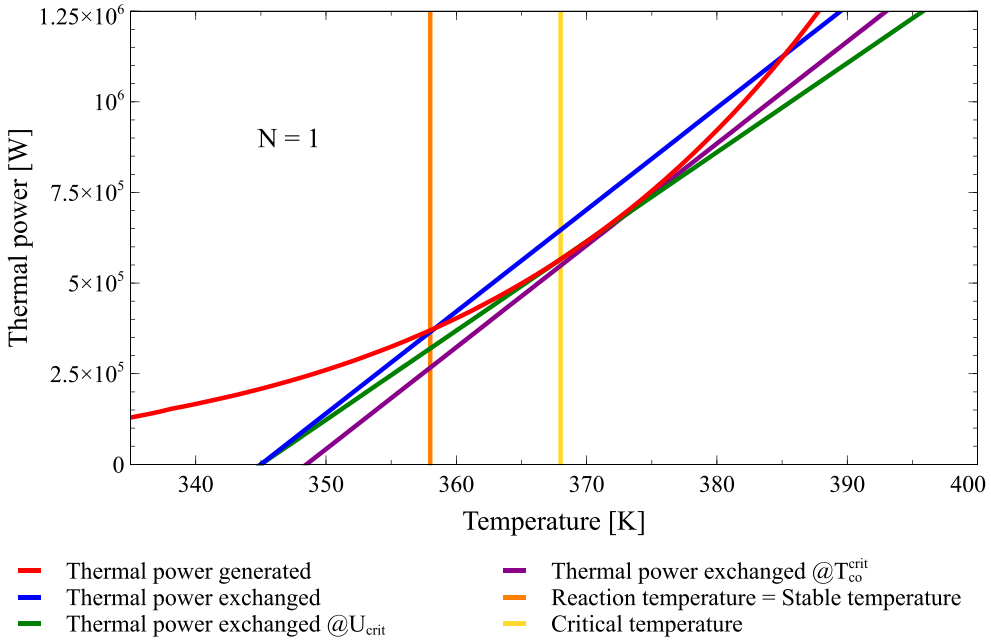

Fig. 7. Semenov's plot for the CSTR belonging to solution 7.

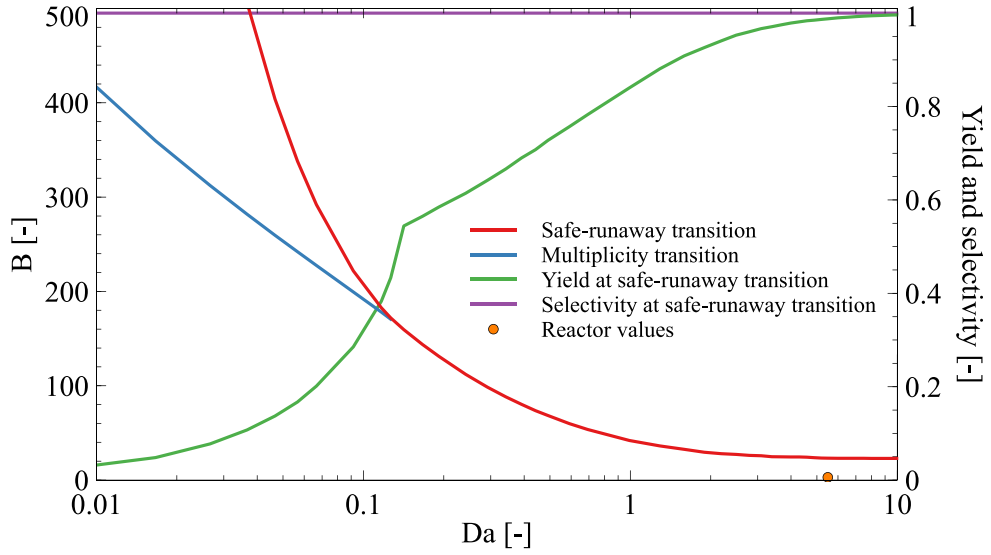

Fig. 8. Reactor operation diagram for the CSTR belonging to Solution 7.

Table 2
Comparison of the results obtainable with different methods.

	$T_{in}[K]$	$T_{out}[K]$	$T_{co}[K]$	$\chi \approx \eta[-]$
ST	–	358	345	0.990
VMWT	345	346.5	345	0.970

to the onset of multiplicity. More specifically, when multiple steady states are feasible, a stable and safe reactor shall operate at the lowest possible reaction temperature. This has a detrimental effect on the reaction rates and, therefore, the obtainable yield. In addition, Table 2 reported results obtained by the implementation of the presented methodology following the Semenov theory or the Varma, Morbidelli, and Wu's theory, respectively.

Even if the different modelling assumptions affect the value of the outlet temperature, mainly because the VMWT can take into consideration the thermal energy of the inlet stream, from the obtained yield is clear that all the methods produce practically the same output. This represents further proof of the agreement between the two design theories involved.

4. Conclusions

The design of innovative and sustainable processes and chemical reactors represents a multidisciplinary task accounting for several technological, safety, environmental, and economic aspects. To reach this target, the present work developed and tested a multi-criteria approach based on fundamental methodologies such as Semenov and Varma, Morbidelli, and Wu's theories. A critical analysis of the available approaches was performed to identify the possible limitations and constraints in applying the abovementioned theories. The gathered information was considered to produce an integrated methodology for identifying and assessing key performance indicators relevant to

chemical reactors.

The developed method was tested for a case study based on the production of vitamin A. A kinetic mechanism was produced to mimic the possible secondary reactions under the operative conditions. The results obtained by the newly developed design method for the case study were validated against data from the literature, allowing for the scale-up from a batch to a continuous process from bench-scale experimental and database information. Different reactor configurations were considered in this analysis. Possible alternative arrangements were designed and evaluated based on the resulting KPIs, optimizing the overall sustainability of the analysed solutions. In conclusion, this work generated and validated an algorithm for a sustainable design of chemical reactors, allowing for preliminary investigations and evaluation of possible alternative solutions.

Declaration of competing interest

The authors declare that they have no known competing financial interests or personal relationships that could have appeared to influence the work reported in this paper.

Data availability

Data will be made available on request.

Appendix A. Supplementary data

Supplementary data to this article can be found online at https://doi.org/10.1016/j.ces.2023.119591.

References

Anastas, P.T., Zimmerman, J.B., 2003. Design through the 12 principles of green engineering. Environ. Sci. Tech. 37 (5), 94A–101A. https://doi.org/10.1021/es032373g.

Awad, H., El-Mewafi, M., Negm, M.S., Gar Alalm, M., 2022. A divided flow aerobic-anoxic baffled reactor for simultaneous nitrification-denitrification of domestic wastewater. Sci. Total Environ. 833, 155247.

Babrauskas, V. (2014). *Ignition Handbook: Principles and applications to fire safety engineering, fire investigation, risk management and forensic science* (2nd ed.). Fire Science Publishers and Society of Fire Protection Engineers.

Bao, Y., Wang, B., Lin, M., Gao, Z., Yang, J., 2015. Influence of impeller diameter on overall gas dispersion properties in a sparged multi-impeller stirred tank. Chin. J. Chem. Eng. 23 (6), 890–896. https://doi.org/10.1016/j.cjche.2014.11.030.

Chansarkar, R., Mukhopadhyay, K., Kelkar, A.A., Chaudhari, R.V., 2003. Activity and selectivity of Rh-complex catalysts in hydroformylation of 1,4-diacetoxy-butene to Vitamin A intermediate. Catal. Today 79–80, 51–58. https://doi.org/10.1016/S0920-5861(03)00044-0.

Chen, W.-H., Lu, C.-Y., Chou, W.-S., Kumar Sharma, A., Saravanakumar, A., Tran, K.-Q., 2023. Design and optimization of a crossflow tube reactor system for hydrogen production by combining ethanol steam reforming and water gas shift reaction. Fuel 334, 126628.

Dai, Y., van Spronsen, J., Witkamp, G.J., Verpoorte, R., Choi, Y.H., 2013. Natural deep eutectic solvents as new potential media for green technology. Anal. Chim. Acta 766, 61–68. https://doi.org/10.1016/j.aca.2012.12.019.

De Liso, B.A., Palma, V., Pio, G., Renda, S., Salzano, E., 2023. Extremely low temperatures for the synthesis of ethylene oxide. Ind. Eng. Chem. Res. 62 (18), 6943–6952. https://doi.org/10.1021/acs.iecr.3c00402.

de Matos, B., Salles, R., Mendes, J., Gouveia, J.R., Baptista, A.J., Moura, P., 2023. A review of energy and sustainability kpi-based monitoring and control methodologies on WWTPs. In *Mathematics* Vol. 11, Issue 1, MDPI. https://doi.org/10.3390/math11010173.

Ebadi, M., Mehrpooya, M., Kani, A.H., 2022. Sensitivity analysis and optimization of geometric and operational parameters in a thermochemical heat storage redox reactor used for concentrated solar power plants. J. Therm. Anal. Calorim. 147 (11), 6415–6435. https://doi.org/10.1007/s10973-021-10980-3.

Ennis, T., 2006. Pressure relief considerations for low-pressure (atmospheric) storage tanks. Inst. Chem. Eng. Symp. Ser. 910–922.

Froment, G. F., Bischoff, K. B., & De Wilde, J. (2011). *Chemical Reactor Analysis and Design* (Inc. John Wiley & Sons, Ed.; 3rd ed.).

Furukawa, H., Kamiya, T., Kato, Y., 2019. Correlation of power consumption of double impeller based on impeller spacing in laminar region. Int. J. Chem. Eng. 2019, 1–7.

Gan, X., Fernandez, I.C., Guo, J., Wilson, M., Zhao, Y., Zhou, B., Wu, J., 2017. When to use what: Methods for weighting and aggregating sustainability indicators. Ecol. Ind. 81, 491–502.

Gao, C.W., Allen, J.W., Green, W.H., West, R.H., 2016. Reaction mechanism generator: automatic construction of chemical kinetic mechanisms. Comput. Phys. Commun. 203, 212–225. https://doi.org/10.1016/j.cpc.2016.02.013.

Hodgett, R.E., 2016. Comparison of multi-criteria decision-making methods for equipment selection. Int. J. Adv. Manuf. Technol. 85 (5–8), 1145–1157. https://doi.org/10.1007/s00170-015-7993-2.

Hutahaean, J., Cilliers, J., Brito-Parada, P.R., 2018. A multicriteria decision framework for the selection of biomass separation equipment. Chem. Eng. Technol. 41 (12), 2346–2357. https://doi.org/10.1002/ceat.201800287.

Iezzi, L., Vilardi, G., Saviano, G., Stoller, M., 2022. On the equipment design of a spinning disk reactor for the production of novel nano silver in amorphous zeolite particles. Chem. Eng. J. 449, 137864.

Jagani, H., Hebbar, K., Gang, S.S., Vasanth Raj, P., Chandrashekhar, R.H., Rao, J.v., 2010. An overview of fermenter and the design considerations to enhance its productivity. Pharmacologyonline 1, 261–301.

Lagerman, C.E., Grover, M.A., Rousseau, R.W., Bommarius, A.S., 2022. Reactor design and optimization of α-amino ester hydrolase- catalyzed synthesis of cephalexin. Front. Bioeng. Biotechnol. 10 https://doi.org/10.3389/fbioe.2022.826357.

Luong, H.T., Volesky, B., 1979. Mechanical power requirements of gas-liquid agitated systems. AIChE J 25 (5), 893–895. https://doi.org/10.1002/aic.690250520.

Martínez-Gómez, J., Narváez, C.R.a., 2016. Material selection using multi-criteria decision making methods (mcdm) for design a multi-tubular packed-bed fischer-tropsch reactor (MPBR). Int. J. Eng. Trends Technol. 34 (6), 273–289. https://doi.org/10.14445/22315381/ijett-v34p255.

Nardo, M., Saisana, M., Saltelli, A., Tarantola, S., 2005. Tools for composite indicators building. JRC Publications Repository. https://publications.jrc.ec.europa.eu/repository/handle/JRC31473.

Parker, G.L., Smith, L.K., Baxendale, I.R., 2016. Development of the industrial synthesis of vitamin A. Tetrahedron 72 (13), 1645–1652.

Paul, E.L., Atiemo-Obeng, V.A., Kresta, S.M., 2004. Handbook of Industrial Mixing Science and practice, (1st ed.). John Wiley & Sons.

Pio, G., Carboni, M., Salzano, E., 2019. Realistic aviation fuel chemistry in computational fluid dynamics. Fuel 254, 115676.

Pio, G., Dong, X., Salzano, E., Green, W.H., 2022. Automatically generated model for light alkene combustion. Combust. Flame 241, 112080.

Pio, G., Salzano, E., 2020. Implementation of gas-phase kinetic model for the optimization of the ethylene oxide production. Chem. Eng. Sci. 212, 115331.

Rabitz, H., Kramer, M., Dacol, D., 1983. Sensitivity analysis in chemical kinetics. Annu. Rev. Phys. Chem. 34, 419–461. https://doi.org/10.1146/annurev.pc.34.100183.002223.

Serna, J., Díaz Martinez, E.N., Narváez Rincón, P.C., Camargo, M., Gálvez, D., Orjuela, Á., 2016. Multi-criteria decision analysis for the selection of sustainable chemical process routes during early design stages. Chem. Eng. Res. Des. 113, 28–49. https://doi.org/10.1016/j.cherd.2016.07.001.

Sheldon, R.A., Arends, I.W.C.E., Ten Brink, G.-J., Dijksman, A., 2002. Green, catalytic oxidations of alcohols. Acc. Chem. Res. 35 (9), 774–781. https://doi.org/10.1021/ar010075n.

Sinnott, R., Towler, G., 2020. Coulson and Richardson's Chemical Engineering Series: Chemical Engineering Design, (6th ed.). Elsevier Ltd.

Torcida, M.F., Curto, D., Martín, M., 2022. Design and optimization of CO2 hydrogenation multibed reactors. Chem. Eng. Res. Des. 181, 89–100. https://doi.org/10.1016/j.cherd.2022.03.007.

Tugnoli, A., Santarelli, F., Cozzani, V., 2008. An approach to quantitative sustainability assessment in the early stages of process design. Environ. Sci. Tech. 42 (12), 4555–4562. https://doi.org/10.1021/es702441r.

Uddin, Z., Yu, B.-Y., Lee, H.-Y., 2022. Evaluation of alternative processes of CO2 methanation: design, optimization, control, techno-economic and environmental analysis. J. CO2 Util. 60, 101974.

Varma, A., Morbidelli, M., Wu, H., 1999. Parametric Sensitivity in Chemical Systems, (1st ed.). Cambridge University Press.

Woods, D.R., 2007. Rules of Thumb in Engineering Practice, (1st ed.). WILEY-VCH.

Wu, Y., Ye, H., Dong, H., guang., 2023. A Multi-objective optimization for batch chemical reaction Processes: the trade-off between economy and safety. Chem. Eng. Sci. 265 https://doi.org/10.1016/j.ces.2022.118231.

Zanobetti, F., Pio, G., Jafarzadeh, S., Ortiz, M.M., Cozzani, V., 2023. Inherent safety of clean fuels for maritime transport. Process Saf. Environ. Prot. 174, 1044–1055. https://doi.org/10.1016/j.psep.2023.05.018.